

POLYCHROMATIC X-RAY MICRODIFFRACTION  
CHARACTERIZATION OF LOCAL CRYSTALLOGRAPHIC  
MICROSTRUCTURE EVOLUTION IN 3D

G.E. Ice and R.I. Barabash

Oak Ridge National Laboratory, Oak Ridge, TN, USA

ABSTRACT

Three-dimensional (3D) spatially resolved characterization of unpaired dislocation-density distributions is conveniently made with polychromatic x-ray microdiffraction. In general, polychromatic microdiffraction provides information about the local subgrain orientation, unpaired dislocation density and elastic strain tensor. This information can be used for direct comparison to theoretical models with matching initial and final conditions. By employing polychromatic x-ray beams and a virtual pinhole camera method, called differential aperture microscopy, 3D distributions of the local crystalline phase, orientation (texture), elastic strain and plastic strain gradient tensor distributions can be measured with submicron resolution in all directions.

1. INTRODUCTION

Although polychromatic Laue Diffraction is the oldest diffraction method it is rarely used to measure strain because the precision of most Laue instruments is low compared to modern diffractometers/goniometers, and because the unit cell volume cannot be determined with a standard Laue measurement. Nevertheless, with suitable instrumentation (Ice 1997), the Laue method can be used to precisely determine the orientation (local texture) of individual grains or subgrains, and their plastic and elastic distortional strain. Laue diffraction can also be extended by measuring the energy of one or more reflections to determine the full strain tensor in polycrystalline samples.

2. EXPERIMENTAL CONSIDERATIONS

Laue diffraction can be visualized by a construction analogous to the Ewald Sphere of monochromatic diffraction. As shown in Fig. 1 the Ewald Sphere is replaced by a

volume in reciprocal space between the lower and upper bounds of the x-ray beam band pass. Reciprocal lattice points that lie in the region bounded by the two shells are effectively scattering and Laue patterns provide radial integrals through reciprocal space weighted by geometric factors, sample absorption and the spectral density distribution (Barabash, Ice, Larson, Pharr, Chung, and Yang 2001). The use of small x-ray beams ( $\sim 500$  nm) immediately restricts the scattering sample volume. This sample volume is adjusted by moving the sample under the fixed x-ray beam. In some cases, (e.g. highly absorbing materials) the scattering volume is further limited to a near-surface region. In other cases (e.g. layered materials) the Laue patterns are distinct for different layers so the 3D position of each pattern can be inferred from the layer order.

Because polychromatic microdiffraction produces Laue images from each subgrain intercepted by the x-ray beam, the typical problem is an overlap of many Laue patterns that must be disentangled. The process of disentangling can be carried out either by a direct experimental technique called differential aperture microscopy (Larson, Yang, Ice, Budai, and Tischler 2002) or by pattern matching/absorption sensitive methods. Once the Laue pattern from a subgrain volume has been obtained and the indices of each reflection determined, powerful single-crystal methods can be employed to determine the unit cell parameters. Although differential aperture microscopy (DAXM) can often resolve Laue images into single crystal-like patterns, when the density of dislocations is high, streaking is observed even in thin films and for DAXM resolved patterns. Typically streaking in Laue patterns indicates the presence of lattice rotations as a result of unpaired or “geometrically necessary” dislocations. However, streaking can also result from gradients in the elastic strain tensor as elegantly illustrated in an experiment by Larson et al. (2002). In cases where both elastic and plastic deformations are present, the elastic contribution must be calculated point-by-point and used to correct the lattice rotations that then are used to calculate the strain gradient tensor. Here we restrict ourselves to cases where elastic contributions are assumed to be negligible. Particularly relevant is the connection to mesoscale deformation structures.

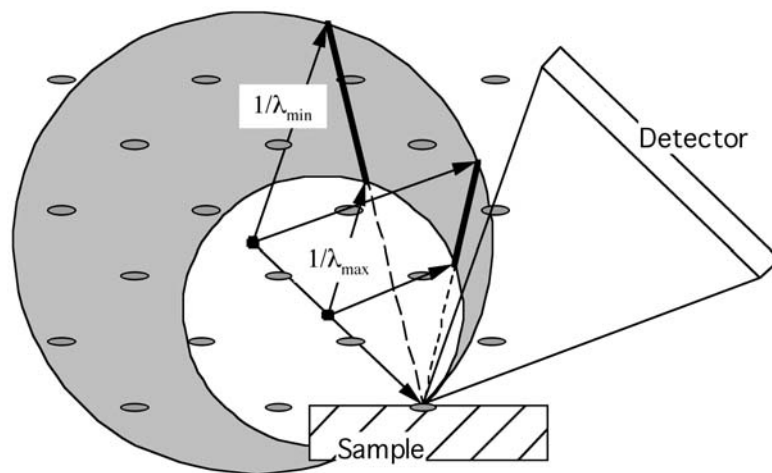


Fig. 1. Ewald sphere for Laue diffraction. Reciprocal space points located between the upper and lower bounds set by the maximum and minimum wavelengths are efficiently reflecting. The Laue image is composed of radial integrals through reciprocal space. Each integral includes weighting from absorption effects, geometrical effects and the incident beam spectral distribution.

### 3. DISLOCATION ARRANGEMENT FROM POLYCHROMATIC DIFFRACTION

A number of experimental studies of plastic deformation under different loading conditions show that typically the cell-wall structure with alternating regions of high and low dislocations density is formed (Pantleon 2002; Hansen 2001; Mughrabi 1983). The dislocation walls contain a high density of dislocations, and cell interiors have very low dislocation population.

**3.1 Misorientation vector.** An approach to characterize the dislocation structure and determine the activated slip systems by analyzing the streaked Laue pattern using a multiscale hierarchical framework is described in detail in (Barabash, Ice, and Walker 2003). In white beam diffraction, the full width at half maximum of the streak  $FWHM \equiv \delta m$  is a function of the misorientation vector  $m$  (rather than the reciprocal space vector for monochromatic beam). To describe the intensity redistribution near a Laue spot, due to a particular set of dislocations, the mutual orientation of two planes are important:

- The plane perpendicular to the direction of dislocation line  $\tau$  in real space;
- The plane perpendicular to the direction of the reciprocal lattice vector  $\mathbf{G}_{hkl}$ .

The line of intersection of these two planes naturally defines the direction of the streak axis  $\xi = \tau \times \mathbf{G}_{hkl} / |\tau \times \mathbf{G}_{hkl}|$ . The second axis  $\nu$  is perpendicular to the  $\xi$  axis and to the reciprocal lattice vector  $\mathbf{G}_{hkl}$ . With this coordinate system, the intensity of a Laue spot is strongly elongated along the  $\xi$  direction. The full width at half maximum in the  $\xi$  direction  $FWHM_{\xi} \equiv \delta m_{\xi}$  depends on the orientation and the number of unpaired or geometrically necessary dislocations (GNDs) in the probed volume. The orientation of the GNDs influences the character of Laue spot. In transverse direction  $\nu$ , the  $FWHM_{\nu} \equiv \delta m_{\nu}$  depends on the total number of all (geometrically necessary and statistically stored) dislocations per unit length and usually  $\delta m_{\xi} \gg \delta m_{\nu}$ .

**3.2 Dislocation density tensor.** According to Nye (1953), the components of the dislocation density tensor can be written as

$$\rho_{ik} = \tau_i b_k \delta(r) \quad (1)$$

The magnitude of the vector  $\tau$  is the net number of dislocations having Burgers vector  $\mathbf{b}$  crossing unit area normal to  $\tau$ . Following the framework of strain gradient plasticity (Gao, Huang, Nix, and Hutchinson 1999), the total density tensor  $\rho_{ij}$  relates to the strain gradient tensor  $\eta_{lmk}$

$$\varepsilon_{ilm} \eta_{lmk} = -\rho_{ik} \quad \eta_{lmk} = \partial^2 u_k / \partial x_l \partial x_m \quad (2)$$

Here,  $\varepsilon_{ilm}$  is the anti-symmetric Levi-Civita tensor. Under multiple slip, the intensity distribution around each reciprocal lattice point and the streak direction  $\xi$  of the Laue spot depends on the aforementioned dislocation density tensor.  $u_k$ , the  $k$  component of the displacement field  $\mathbf{u}$  for any unit cell, is due to all dislocations in the crystal.

3.3 Statistical description of diffraction by dislocations. We calculate the total displacement of the  $i$ -th cell  $\mathbf{u}_i$  from the equilibrium positions  $\mathbf{R}_i^0$  corresponding to the undeformed crystal using continuum elastic theory. This displacement

$$\mathbf{u}_i = \sum_t c_t \mathbf{u}_{it} \quad (3)$$

is due to all dislocations and defined using random numbers  $c_t$  (Barabash et al. 2001; Barabash et al. 2003), with  $c_t=1$ , if there is a dislocation at position  $t$ , and  $c_t=0$  for positions without dislocations. The plain-strain bending of a crystal of curvature  $K$  is usually modelled by a network of randomly distributed geometrically necessary dislocations with density  $n^+$  and Burgers vector  $\mathbf{b}$ . For example, the Cartesian reference frame is set such that the  $x_1$  axis coincides with the direction of the Burgers vector  $\mathbf{b}$  and  $x_3$  coincides with the direction of dislocation lines of the dislocation net. With this coordinate system the crystal will be bent in the plane  $x_1x_2$  due to the net of GNDs. In this Cartesian reference frame the only nonzero components of the dislocation density tensor is  $\rho_{31}$  resulting in the nonzero components of the strain gradient tensor:  $\eta_{112} = -K$  and  $\eta_{211} = K$ , with an effective strain gradient  $\eta = K = n^+b$ .

3.4 Simulations. The component  $\rho_{ik}$  of the dislocation density tensor gives the sum of the Burgers vectors of all dislocations whose Burgers vector and line direction are directed parallel to  $x_k$  and  $x_i$  axes, respectively. These are set as an initial input parameter for simulations of the Laue pattern. By simulating Laue images with different GND slip systems, we can determine the set of slip systems that fit best to the local lattice curvature and experimentally determined Laue images. The analysis of the dislocation substructure for multiple slip deformation includes the following steps:

- Determination of the local lattice curvature (misorientation axes and angle) from the experimental Laue pattern at each probed location.
- Simulation of Laue pattern using these parameters to check its identity with the original experimental image.
- Performing least square fit of the streak profile to find the components of the dislocation density tensor.

3.5 Dislocation arrangement in the heat affected zone of an Ir weld. As an example, we describe the analysis of microbeam Laue diffraction from an Ir weld. Experimental details have been described in detail by Ice and Larson (2002). Ir weld samples are relatively easy to analyze with microdiffraction because only one or two grains are probed simultaneously; even 20 keV x-rays only penetrate couple of microns into iridium. Although this limits the recovered information to the near surface region it probes many orders of magnitude further into the sample than traditional surface probes. It is well known, that contraction of the molten weld metal during solidification is resisted by the surrounding metal, resulting in the appearance of stresses (Noyan and Cohen 1987). These stresses may partially relax by plastic deformation. As shown in the Laue patterns (Fig. 2), welding of polycrystalline Ir is accompanied by local plastic deformation as well as by residual stress. Microbeam Laue diffraction reveals pronounced streaking of the Laue images from grains in the heat affected zone (HAZ). The plastic response of the material in the HAZ can be described by the formation of

GNDs that appear in the material to relax the stress field induced during welding and subsequent cooling.

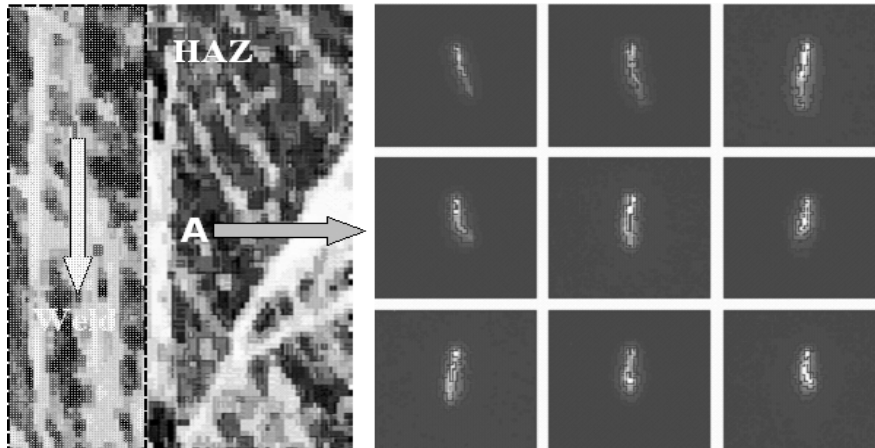


Fig. 2. Optical photomicrograph of an Ir weld (left) and  $\bar{1}14$  Laue reflection for 9 neighboring positions displaced in  $3\ \mu\text{m}$  step in grain A (right).

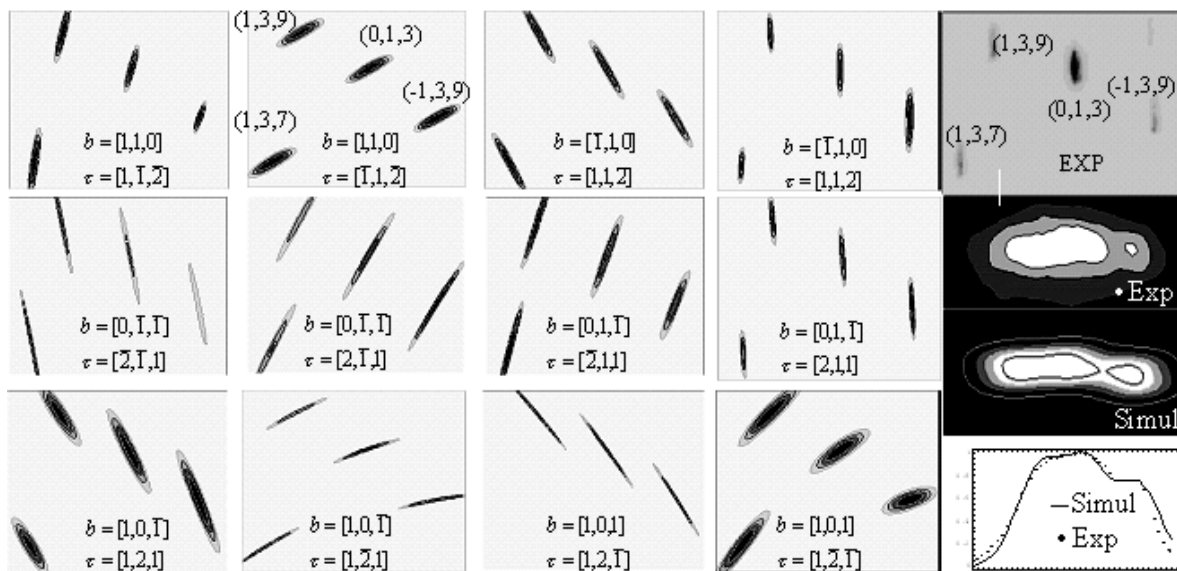


Fig. 3. Different slip systems produce distinct Laue patterns. In this figure the central part of an experimental Laue pattern with 139, 137, 013,  $\bar{1}39$  Laue spots is calculated for edge dislocations systems. The twelve systems are defined by the Burgers vector  $\mathbf{b}$  and dislocation line  $\boldsymbol{\tau}$ . The pattern in the upper right corner is indexed. Contrast factors change the length and width of the streaks. Experimental and simulated contour maps of one Laue spot and slices of intensity along the streak direction are shown in the right column.

In face centered cubic crystals, typical edge dislocation lines with Burgers vectors parallel to  $\langle 110 \rangle$  “run” parallel to  $\langle 112 \rangle$  on the corresponding glide planes  $\{111\}$  (Nabarro 1967). There are twelve such systems for each crystal grain. To understand the shape of experimental Laue images and to check the sensitivity of the Laue image to different possible dislocation kinds, we have chosen four reflections closest to the center of the Laue pattern 139, 137, 013,  $\bar{1}39$  for grain A in the HAZ (Fig. 3). We

simulated their Laue images corresponding to twelve different slip systems of the primary GNDs (Figs. 3). The twelve edge dislocation systems for grain A in the sample contribute with distinct patterns to the beam spread. Analysis of those images indicates that only two of the slip systems (the two top ones on the right hand side) give images that are close to the experimental one. Further analysis is performed by simulation of the whole Laue pattern for the above three possible slip systems. Performing least square fit to find the predominant slip systems corresponding to the dislocation density tensor we determined the direction of the activated slip system in different depth regions and simulated Laue images corresponding to the best fit slip system parameters.

In this sample, the overall streaking direction fluctuates but maintains a similar qualitative behavior over most of the grains. Correlated fluctuations in streaking are observed in regularly spaced slip bands. The overall deformation behavior is highly correlated with the crystallographic orientation of the weld and with the thermal gradients. In average, it results in lattice misorientations in the HAZ primarily around the axis perpendicular to the weld direction.

#### ACKNOWLEDGEMENTS

This research is supported by the U.S. DOE, Basic Energy Sciences, Office of Science under contract DE-AC05-00OR22725 with UT-Battelle LLC. Measurements were made on Unicat beamline ID-34-E at the APS also supported by DOE office of science.

#### REFERENCES

- Barabash, R., Ice, G.E., Larson, B.C., Pharr, G.M., Chung, K.S., and Yang, W. (2001). White microbeam diffraction from distorted crystals. *Appl. Phys. Lett.* 79, 749-751.
- Barabash, R.I., Ice, G.E., and Walker, F.J. (2003). Quantitative microdiffraction from deformed crystals with unpaired dislocations and dislocation walls. *J. Appl. Phys.* 93, 1457-1464.
- Gao, H., Huang, Y., Nix, W.D., and Hutchinson, J.W. (1999). Mechanism-based strain gradient plasticity - I. Theory. *J. Mech. Phys. Solids* 47, 1239-1263.
- Hansen, N. (2001). New discoveries in deformed metals. *Metall. Mater. Trans. A* 32, 2917-2935.
- Ice, G. E. (1997). Microbeam-forming methods for synchrotron radiation. *X-Ray Spectrometry* 26, 315-326
- Ice, G.E., and Larson, B.C. (2002). 3D x-ray crystal microscope. *Adv. Eng. Mater.* 2, 643-646
- Larson, B.C., Yang, W., Ice, G.E., Budai, J.D., and Tischler, J.Z. (2002). Three-dimensional x-ray structural microscopy with submicrometer resolution. *Nature* 415, 887-890.
- Mughrabi, H. (1983). Dislocation wall and cell structures and long-range internal stresses in deformed metal crystals. *Acta metall.* 31, 1367-1379
- Nabarro, F.R.N. (1967). *Theory of crystal dislocations* (New York, Dover Publications).
- Noyan, I.C., Cohen, J.B. (1987) *Residual stress* (Springer-Verlag, New York).

## Polychromatic x-ray microdiffraction characterization

- Nye, J.F. (1953). Some geometrical relations in dislocated crystals. *Acta Metall.* 1, 153-162.
- Pantleon, W. (2002). Disorientations in dislocation structures: formation and spatial correlation. *J. Mater. Res.* 17, 2433-2441.